Efficiency of layered double hydroxides in epoxy coating as corrosion inhibitor reservoirs for carbon steel

G. J. Ayemi, C. Blivet, S. Marcelin, S. Therias, F. Leroux, B. Normand

▶ **To cite this version:**

G. J. Ayemi, C. Blivet, S. Marcelin, S. Therias, F. Leroux, et al.. Efficiency of layered double hydroxides in epoxy coating as corrosion inhibitor reservoirs for carbon steel. Applied Clay Science, 2024, 258, pp.107510. ⟨10.1016/j.clay.2024.107510⟩. ⟨hal-04672843⟩

HAL Id: hal-04672843

https://hal.science/hal-04672843v1

Submitted on 6 Nov 2025

HAL is a multi-disciplinary open access archive for the deposit and dissemination of scientific research documents, whether they are published or not. The documents may come from teaching and research institutions in France or abroad, or from public or private research centers.

L'archive ouverte pluridisciplinaire **HAL**, est destinée au dépôt et à la diffusion de documents scientifiques de niveau recherche, publiés ou non, émanant des établissements d'enseignement et de recherche français ou étrangers, des laboratoires publics ou privés.

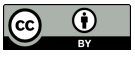

Distributed under a Creative Commons CC BY 4.0 - Attribution - International License

Efficiency of Layered double hydroxides in epoxy coating as corrosion inhibitor reservoirs for carbon steel

G. J. Ayemi[a], C. Blivet[b], S. Marcelin[a*], S. Therias[b], F. Leroux[b], B. Normand[a]

[a] *Univ. Lyon, INSA Lyon, Université Claude Bernard Lyon 1,*

CNRS, MATEIS, UMR5510, 69621 Villeurbanne, France

[b] *Université Clermont-Auvergne-CNRS-UMR 6296, ICCF F-63178 Aubière, France*

Abstract

Layered double hydroxides (LDHs) are considered as interesting containers for corrosion inhibitors, since they exhibit high ability to release inhibitor as well as to capture aggressive ions from aqueous solution. Epoxy containing organo-modified LDHs filler intercalated with ethylenediamine-N,N'-disuccinate anions (EDDS), $[Zn_2Al(OH)_6]^+ [EDDS]^{4-}_{0.25} . 2H_2O$ (LDH-EDDS) with loading from 0 % to 1.25 % were coated onto carbon steel plates. The efficiency of these coatings against corrosion (barrier properties and release of inhibitors) was assessed by using electrochemical impedance spectroscopy. The evolution of the impedance modulus |Z| at low frequency range during time showed that the 0.75% organo-modified LDH-containing epoxy (thickness 80 µm) exhibits the highest corrosion resistance in the series and the associated value of |Z| at 3 mHz (10^{10} Ω cm^2 after 21 days of immersion in 0.1 M NaCl solution) places it among the best recent solutions published now. The behavior of this polymer composite was compared to the free-LDH coating by plotting the resistivity profiles along the coating thickness as a function of time. These results show that (*i*) the presence of 0.75 % LDH-EDDS in the epoxy coating delays the penetration of water molecules, and (*ii*) limits corrosion of carbon steel. The efficiency of the organo-modified filler to inhibit the corrosion process is explained by an exchange between interleaved species occurring from released $EDDS^{4-}$ anions and aggressive Cl^- ions being captured.

Keywords: Corrosion inhibition, Carbon Steel, Epoxy coating, LDH, EIS

*Corresponding author: sabrina.marcelin@insa-lyon.fr

1. Introduction

Layered Double Hydroxides (LDHs) are composed of layers of edge-sharing octahedral of metal hydroxides, which may be of different nature, with an anion intercalated between them. This anion can be exchanged by another anion, this by mass action law and/or affinity allowing their diffusion within the host structure (Tedim et al., 2012; Alibakhshi et al. 2017; Cao et al., 2022a; Seniski et al., 2020;). This is particularly relevant concerning corrosion issues when suitable anions are then released by such exchange process associated with the capture of chloride ions (Poznyak et al., 2009; Hang et al., 2010; Zheludkevich et al., 2010; Hang et al., 2012; Tabish et al., 2021; Ayemi et al., 2022; Cao et al., 2022a). The latter is known to be aggressive towards metal surface. Thus, LDHs can be considered as inhibitor reservoirs, where the inhibiting species is the anions initially intercalated between the hydroxide layers (Junaid et al., 2020; Leal et al., 2020; Wei et al., 2020; Pellanda et al., 2021). They migrate out of the filler structure into the solution until being adsorbed onto the metal surface by forming some organometallic compound with the metal ions resulting from the metal oxidation process (Fig. 1) (Zheludkevich et al., 2010; Hang et al., 2012; Tabish et al., 2021; Ayemi et al., 2022; Cao et al., 2022a; Hejjaj et al., 2024).

In previous work, LDHs constituted of zinc and aluminium hydroxides layers intercalating Ethylenediamine-N,N'-disuccinate anions ($EDDS^{4-}$) were synthetized to evaluate the inhibitive efficiency of this hybrid compound on carbon steel reactivity in neutral and aerated 0.1M NaCl solution (Ayemi et al., 2022). It was shown the inhibitive efficiency provided both from an anion exchange mechanism between $EDDS^{4-}$ and Cl^- (Fig. 2) anions to a partial and rather selective solubility of the LDH scaffold leading to the presence of zinc in the solution. This demonstration provides a very interesting opening for the application of organic coatings. In fact, they offer a solution for improving the corrosion resistance of metals

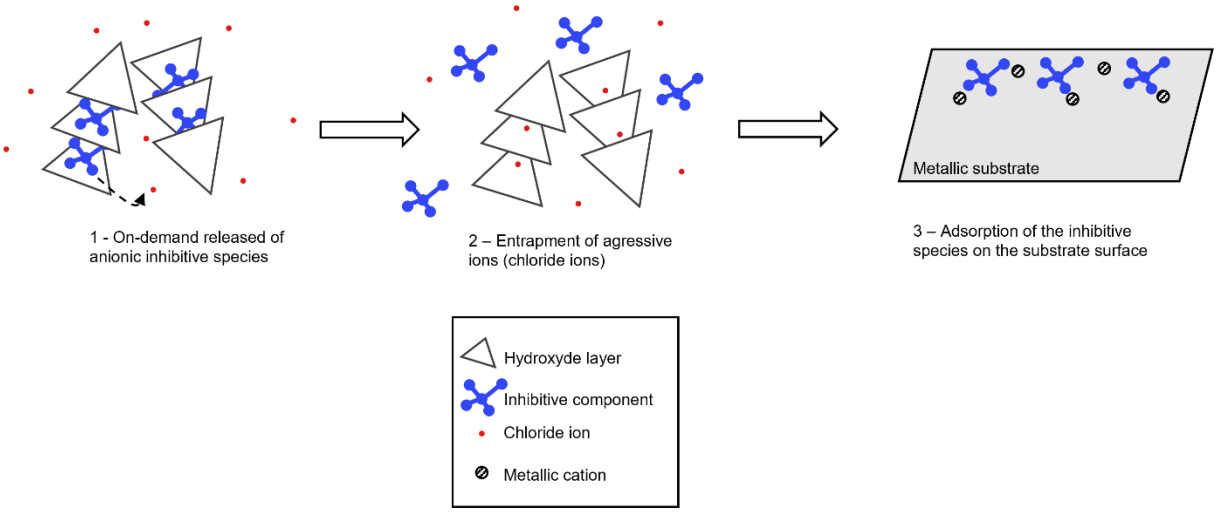

Figure 1: Illustration of the anion exchange process occurring between intercalated anions in the LDH structure and chloride ions from the external environment leading to the adsorption of inhibitor species onto the metal surface.

when it is simply necessary since the cure is caused by corrosion attack (Nguyen et al., 2018; Peng et al., 2018; Su et al., 2020; Udoh et al., 2022; Bakhtaoui et al., 2021; Montemor, 2024). The performance of organic coatings is defined, among other properties, by their barrier properties, which prevent or delay the ingress of water. Barrier properties depend on the tortuosity of the polymer network. However, porous epoxy coatings are damaging to the underlying metal, since water and other aggressive species (chloride ions, oxygen, etc.) can reach the substrate and lead to corrosion. Epoxy coatings incorporating LDHs appear to be an interesting way of inhibiting corrosion (Nguyen et al., 2018; Peng et al., 2018; Asadi et al., 2019; Zhang et al., 2019). In addition, barrier « passive » properties can also be improved by increasing the tortuosity within the polymer network through the addition of these anisotropic compounds (Cao et al., 2021; Sun et al., 2021; Tabish et al., 2021; Cao et al., 2022a).

The present study deals with the characterization of the barrier properties offered by the layered double hydroxide $[Zn_2Al(OH)_6]^+[EDDS]^{4-}_{0.25}$. $2H_2O$ loaded at different concentrations (0 %, 0.25 %, 0.75 % and 1.25 %) in an epoxy matrix. The aim is to validate

the use of these LDHs as inhibitor compounds incorporated in epoxy coating and to determine the best coating formulation associated with a suitable concentration of LDH-EDDS needed for a long-term protection against the corrosion of XC38 carbon steel. The barrier properties are investigated by electrochemical impedance spectroscopy. This technique is relevant because it enables to assess the corrosion resistance of the coated system at the carbon steel/coating interface, and to establish the link between the electrochemical behavior of the coated system and the dielectric properties of the organic matrix, which can be modified by water uptake (Amand et al., 2013; Musiani et al., 2014; Nguyen et al., 2015; Nguyen et al., 2016; Nguyen et al., 2017; Garden and Pethrick, 2017; Marcelin et al., 2023).

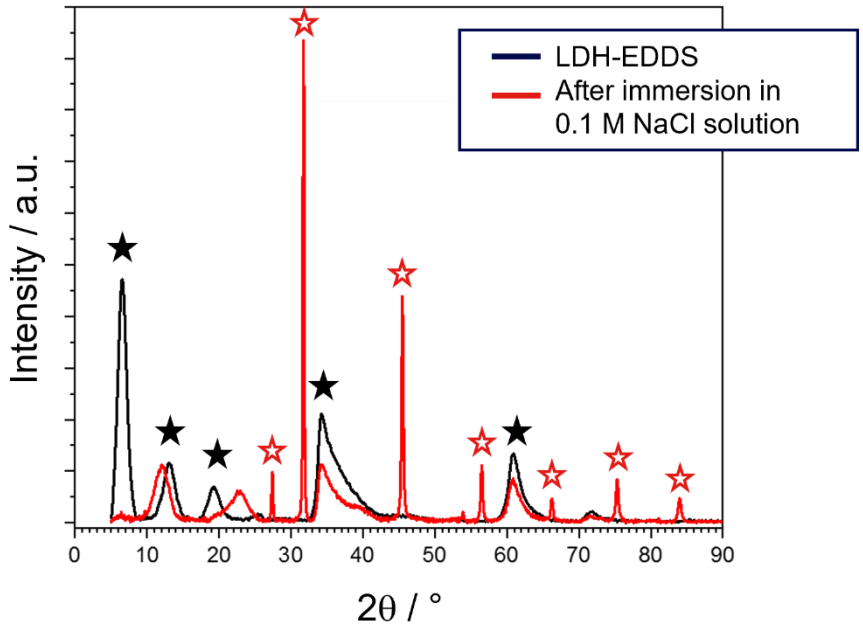

Figure 2: XRD patterns for LDH-EDDS before and after contact with sodium chloride solution showing the exchange reaction between $EDDS^{4-}$ and Cl^- anions, data from (Ayemi et al., 2021).

2. Experimental part

2.1. Preparation of epoxy incorporated LDH-EDDS coatings deposited on XC38 carbon steel

The XC38 carbon steel (C = 0.32-0.39, S ≤ 0.035, Mn = 0.5.-0.80, P ≤ 0.035, Si = 0.40 max, Fe to 100, in wt.%) plates with dimensions 100 x 70 x 3 mm^3 was used as a substrate. The carbon steel plates were sand blasted to a roughness of about 3µm and have been degreased with ethanol prior to the coating deposition to promote adhesion of the coating to the substrate.

The LDH-EDDS used in this study were prepared at room temperature by direct co-precipitation method using the protocols described in our previous work in which, the $EDDS^{4-}$ anion was intercalated between layers of the LDH-type host structure of cation composition Zn_2Al (Ayemi et al., 2021). The chemical structure of EDDS is recalled in figure 3. The powder form of LDH-EDDS was used for the coating formulation.

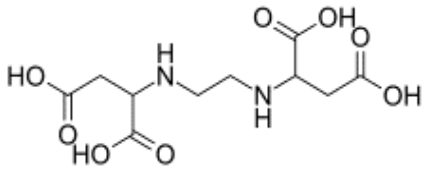

Figure 3: Chemical structure of Ethylenediamine-N,N'-disuccinic acid (EDDS).

Epoxy and epoxy/LDH-EDDS coatings were prepared using an epoxy resin: bisphenol A diglycidyl ether (DGEBA) from Huntsmann (Araldite GZ7071X75) in xylene (at 75%) and a polyamidoamine hardener as the curing agent, from Huntsmann (Aradur 423XW60) in xylene/n-butanol 4:1 (at 60%) solution.

Different percentage weight concentrations (0.25 %, 0.75 % and 1.25 %) of LDH-EDDS grounded to a powder form were mixed with epoxy resin. These concentrations were chosen to determine the best coating formulation and the optimum amount of LDH-EDDS needed for better corrosion protection of XC38 carbon steel. The amine curing agent was then added with the amine/epoxy ratio equal to 1.1. The mixed coating formulation was deposited on XC38 plates using bar coater. The curing protocols were as follows: (*i*) 24 h at room temperature in

the bar coater chamber, to allow slow evaporation of solvent; (*ii*) 1 h at 80 °C in the oven, was the real curing step; and (*iii*) 2 h at 100 °C under vacuum, to ensure maximum curing without early degradation of the coatings. The particle dispersion was checked by Scanning Electron Microscopy (SEM), and particle aggregates of less than 10 µm were observed. Epoxy coating without LDH-EDDS was also produced as reference. The resulting coatings were: Epoxy/amine + 0 % LDH-EDDS, Epoxy/amine + 0.25 % LDH-EDDS, Epoxy/amine + 0.75 % LDH-EDDS, and Epoxy/amine + 1.25 % LDH-EDDS which will be subsequently referred to as 0 %, 0.25 %, 0.75 % and 1.25 % coating, respectively. The expected coating thicknesses were 80 µm. The measured thicknesses using a profilometer showed that the thicknesses were not homogeneous on all the steel plates. The thicknesses of 80 µm ± 5 µm were only reached on a surfaces of a few cm^2 in the center of the samples.

2.2. Analytical characterizations

Differential scanning calorimetry (DSC) measurement was used to determine the glass transition temperature (T_g) of epoxy coatings before immersion. DSC was performed using a Mettler Toledo DSC3+ device at a rate of 15 °C.min^{-1} in the range -20°C to 100°C under air flow. Glass transition temperatures (T_g) were determined from midpoint of the heat flow derivative using STARe software from Mettler Toledo.

2.3. Electrochemical impedance spectroscopy (EIS) of coated systems

The electrochemical measurements were carried out using two cell configurations: carbon steel/coating/mercury (dry condition) and carbon steel/coating/0.1 M NaCl solution (wet condition). In both cases, the coated carbon-steel plate was used as the working electrode. Electrochemical measurements in dry conditions provide the coating permittivity required to calculate water uptake. Electrochemical measurements under wet conditions monitor the evolution of the barrier properties of the epoxy coatings and the corrosion resistance of coated

carbon steel. For the dry condition, the electrochemical cell was filled with mercury (Nguyen et al., 2017). The working electrode had an exposed area of 3 cm², and the platinum wire used as the counter and reference electrode was dipped in mercury to ensure electrical contact. A potentiostat/galvanostat (Biologic SP-300) was used to measure the impedance for this configuration. The impedance diagrams were obtained using a DC bias of 0 V over the frequency range of 10^4 Hz to 0.1 Hz with 8 points per decade and 50 mV RMS peak-to-peak sinusoidal perturbation amplitude. For the wet condition, a three-electrode cell was used. Two different types of masks providing from GAMRY were used to delimit the analysis area to 15 cm² or 3 cm² (the exposure area is the area where the homogeneous coating thickness is 80 µm ± 5 µm). The reference electrode was saturated calomel electrode (SCE), and a graphite porous bar (with a large surface) was used as the counter electrode. Both electrochemical set-ups were placed in a Faraday cage. A potentiostat/galvanostat (Gamry Reference 600) was used to measure the impedance for the carbon steel/coating/electrolyte configuration. The impedance diagrams were obtained under potentiostatic conditions at the corrosion potential over the frequency range of 10^5 Hz to 3 mHz with 8 points per decade and 15 mV RMS peak-to-peak sinusoidal perturbation amplitude. All the impedance measurements were performed at room temperature. For the wet condition, the impedance of the coatings was measured for exposure times ranging from 2 hours to 21 days. The solution was aerated and stagnant during the experimentation. For reproducibility, all measurements were repeated at least three times. The impedance diagrams were analyzed using non-commercial software developed at the LISE UMR CNRS 8235, Paris.

3. Results and discussion

3.1 Dielectric properties of coating under dry condition

The electrochemical impedance was measured in the dry condition to determine the parameters associated with the dielectric properties of the coating (Normand et al., 2004; Nguyen et al., 2017). Figure 4 shows the impedance diagrams obtained for different amounts of LDH in organic matrix. Regardless the content of additive in the epoxy matrix, the phase angle is close to -90° between 10 kHz and 100 Hz. For lower frequencies, a slight distribution of the time constant can be attributed only to the surface roughness (Nguyen et al., 2015).

In parallel, the impedance modulus at lowest frequency is high and close to 10^{11} Ω cm². The results indicate that the coating/mercury interface can be considered as a pure capacitance.

The complex capacitance is given in equation 1. Figure 5 shows the complex capacitances in a Cole-Cole plot for the four samples. The capacitance of the dry coatings was extracted by graphical method (C_∞ indicated in Fig. 3) (Benoit et al., 2016; Chakri et al., 2017) and is reported in the table 1.

$$C(\omega) = \frac{1}{j\omega(Z-R_e)} \quad (1)$$

with, ω the angular frequency ($\omega=2\pi f$), Z the impedance of the coating, and R_e the electrolyte resistance. From the figure 4, the electrochemical behavior of the coated sample (between 10^4 Hz and 10^2 Hz) can be considered as a pure capacitive behavior. Thus, the real part of the capacitance determined at high frequency (C_∞) range allows to obtained the permittivity of the coating given by equation 2.

$$C_\infty = \frac{\varepsilon_c \varepsilon_0}{\delta} \quad (2)$$

with ε_c the permittivity of the dry coating, ε_0 the vacuum permittivity, and δ the coating thickness.

The obtained capacitance and permittivity values are reported in the table 1. The values of the dry coatings obtained are closed to the ones reported in literature (Bouvet et al., 2014; Nguyen et al., 2016). Regardless of LDH-EDDS content, the capacitance values of the coatings are of

the order of 3 to 5 10^{-11} F cm^{-2}, leading to permittivity values of the order of 3 and 4. Note that the T_g are not depending on the content in LDH-EDDS as the values were between 54°C and 57°C (table 1). These values concern organic matrix only which have been submitted to the curing protocols. Since the T_g depends on the cure temperature (Garden and Pethrick, 2017), these closed values characterize that organic matrix are chemically equivalent whatever the presence of LDH.

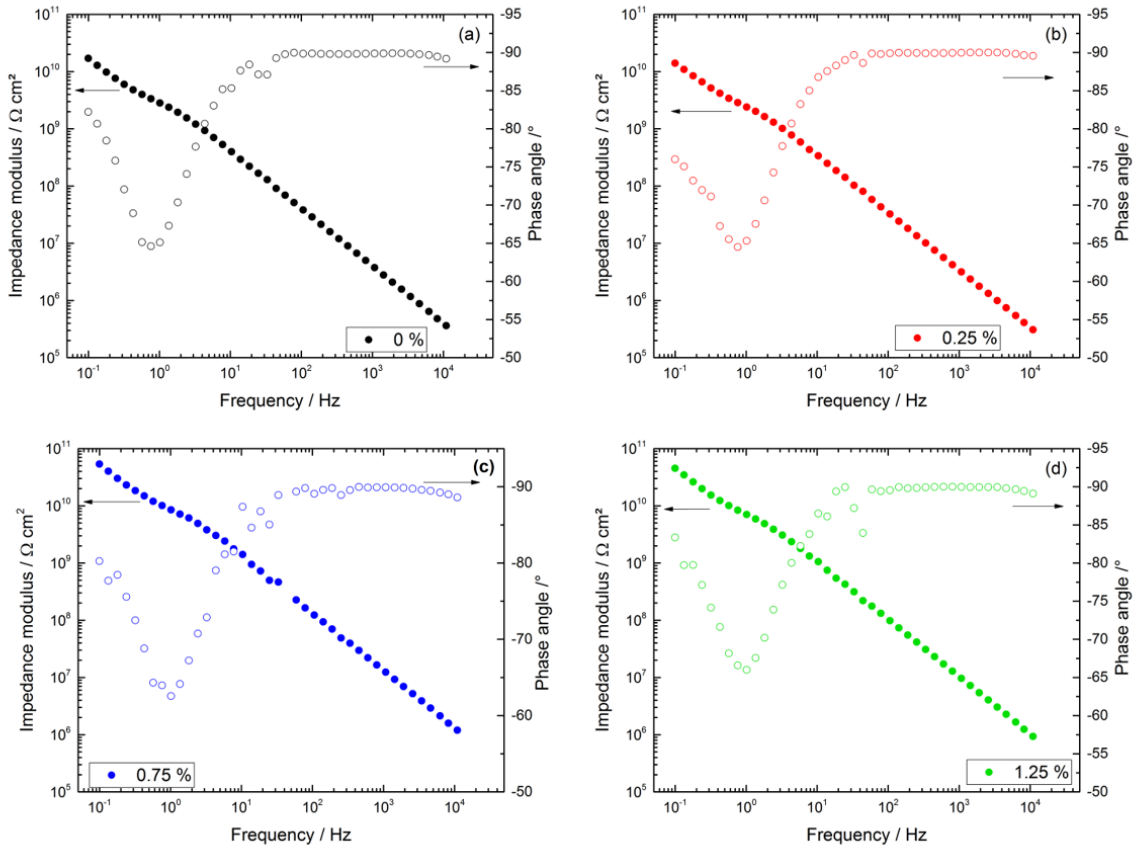

Figure 4: Electrochemical impedance diagrams obtained in dry conditions for the four samples with different contents of LDH: (a) 0 %, (b) 0.25 %, (c) 0.75 % and (d) 1.25 %.

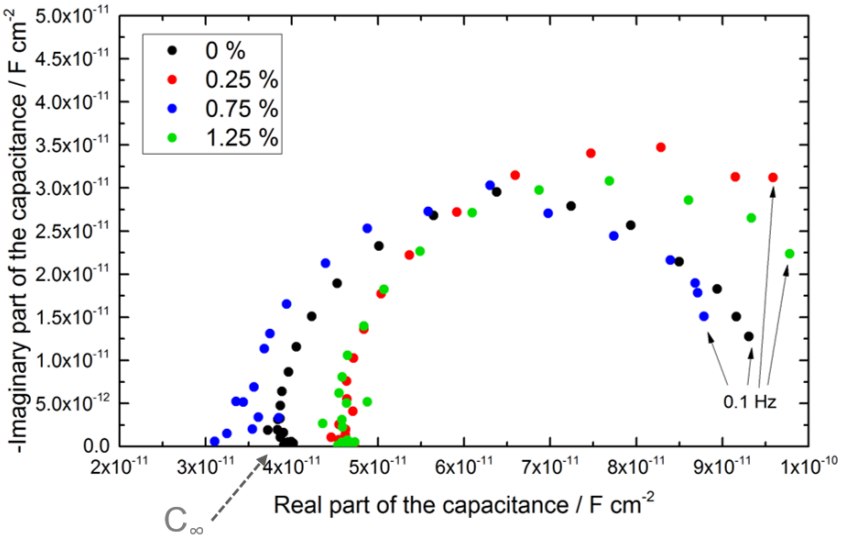

Figure 5: Representation of the experimental data obtained in dry condition (from Fig. 4) in a complex capacitance plane. An example of the C_∞ (representing the coating capacitance) value obtained by the intersection with the real axis is given.

Table 1: Parameters obtained in dry conditions for the different samples

Coatings	C_∞ / 10^{-11} F cm^{-2} *graphically determined from fig. 5*	ε_C *calculated from (eq.2)*	T_g / °C
0 %	3.90	3.5	57
0.25 %	4.63	4.2	57
0.75 %	3.54	3.2	57
1.25 %	3.07	2.8	54

3.2. Evaluation of the electrochemical behaviour of carbon steel/epoxy coating/electrolyte interface

The four coated samples were immersed in the 0.1 M NaCl solution and the impedance was measured during immersion at corrosion potential. Figure 6 presents the evolution of the impedance modulus at 3 mHz during time. This value is representative of the corrosion

resistance of the coated carbon steel (Wang et al., 2018). The evolutions are not the same for all samples. Some of the tests were stopped whenever corrosion signs are noticed, except for the reference coating (without LDH) which was removed at the same immersion time than the 0.75% LDH containing coating. This monitored immersion test was carried out in order to select the best candidate to protect the carbon steel against corrosion. It is interesting to underline that the value of the impedance modulus at low-frequency is not the same for all coatings at the initial time of immersion. For both 0.25% and 0.75% LDH-containing coatings, $|Z|_{3mHz}$ is around 10^{11} Ω cm^2 for the first days of immersion. After 3 days of immersion, for the 0.25%-LDH-containing coating, this value drastically decreases to reach around 5.10^7 Ω cm^2. This value is the same as that reached at the start of immersion for the coating with the highest LDH content, indicating defects in the epoxy matrix and a loss of protection giving rise to a corrosion process underneath the coating (Peng et al., 2020; Yeganeh et al., 2019). The evolution of the impedance modulus at low frequency for the 0.75%-LDH coating is slower and reaches 10^{10} Ω cm^2 after 21 days of immersion.

The comparison with either LDH filler $Zn_2Al:NO_3^-$ or $Zn_2Al:CO_3^{2-}$ was not possible because the particles aggregate themselves into the epoxy resin resulting in a highly heterogeneous surface showing large pieces of inorganic particles badly embedded into the polymer. Such particle aggregation caused coating failure and the impedance tests were not possible to perform because of the rapid passage of the solution beneath the coating. Some tests had shown very poor |Z| at 10^{-2}Hz much lower than the epoxy coating itself, thus suppressing any benefits of having a corrosion inhibitor.

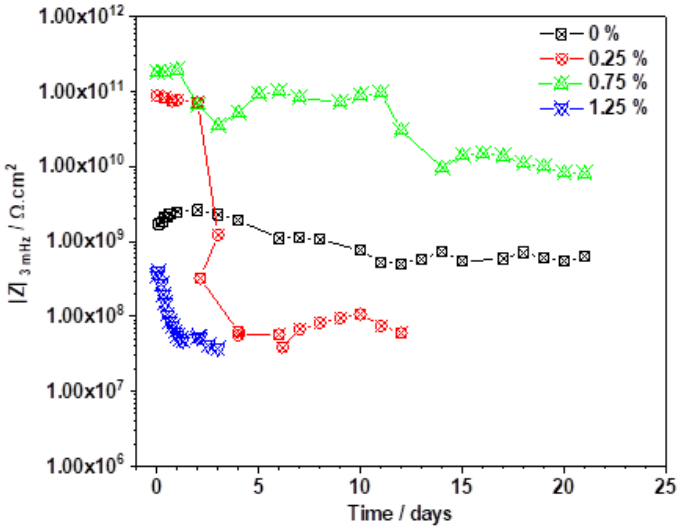

Figure 6: Impedance modulus at 3 mHz for the carbon steel epoxy coated samples with or without LDH-EDDS as a function of immersion time in the neutral chloride electrolyte.

To compare the performance of Zn_2Al:EDDS to other LDH cargos either embarking inhibitor species or mixed with other compounds, a selection of the most recent use of LDH filler for epoxy coating is summarized in Table 2. Two main data are reported when available: the charge transfer resistance R_{CT} obtained after EIS fit with an electrical equivalent circuit since it is related to the electrochemical corrosion reaction and the value of the impedance modulus at low frequency as it measures the physical barrier effect of the coating.

Table 2. Selection of the most recent LDH filler used in epoxy coating, where the cation LDH composition is indicated, the interleaved guest acting as corrosion inhibitor and its associated loading rate, the coating thickness, the impedance modulus |Z| at low frequency as well as the charge transfer resistance R_{CT} when available.

LDH cargo $M^{2+}_nM^{3+}$	Interleaved species *(in combination with)*	Loading rate / wt. %	Coating thickness / µm	Substate	R_{CT} / $\Omega.cm^2$	$\lvert Z\rvert_{10\text{-}2Hz}$ / $\Omega.cm^2$	Ref.
Ca_2Al	NO_2^-	2	120 ± 20	Carbon steel	9.10^{11}	$\approx 10^{12}$	Xue (2023)
Mg_2Al	NO_2^-	0.05	50 ± 5	Q235 steel	-	$\approx 10^8$	Su (2020)
Ca_2Al	NO_3^-	2	-	Steel	-	$\approx 10^7$	Cao (2022b)
Zn_2Al	NO_3^-	2	-		-	$\approx 10^6$	
Mg_2Al	NO_3^-	2	-		-	$\approx 10^4$	
Zn_2Al	Gallate ($C_7H_5O_5^-$)	1	-	Q235 steel	-	$\approx 10^8$	Fang (2023)
Mg_2Al	Fumarate	1	160	Tinplate	$\approx 3.10^5$	$\approx 10^6$	Zhang (2023)

	($C_4H_2O_4^{2-}$)						
Mg_2Al	Molybdate (Gr@PMIH)[a]	0.5	-	Carbon steel	-	10^9	He (2024)
Ca_2Al	2MBT[b]	2	-	Q235 steel	5. 10^7	6.10^7	Tabish (2022)
Zn_2Al	DEDTC[c] ($C_5H_{10}NS_2^-$) (+Mmt (Ce)[d]	-	90 ± 2	AA 2024-T3	-	$\approx 10^9$	Mohammadi (2022)
Mg_2Al	BTA[e] ($C_6H_5N_3$)	1.5	-	Zn-Mg steel	-	$\approx 10^9$	Rodriguez (2020)
Zn_2Al	PSA[f]	0.6	40 ± 2	Carbon steel	-	$\approx 10^{10}$	Ding (2023)
Mg_2Al	MoO_4^{2-} (with $Ti_3C_2T_x$)[g]	0.1	110	P110 steel	-	3.10^8	Li (2023)
Zn-LSH + Zn_2Al	(M+G)[h]	5	50	AISI 1020 carbon steel	-	2.10^8	Leal (2023)
Zn_2Al	EDDS	0.75	80 ± 5	XC38	-	2.10^{11}	This work

[a] Gr@PMIH represents Mg_2Al interleaved with molybdate anion MoO_4^{2-} with polydopamine and onto graphene; [b] 2MBT = 2-mercaptobenzothiazole; [c] DEDTC = diethyldithiocarbamate; [d] Mmt(Ce) montmorillonite loaded with Ce^{3+} cations; [e] BTA benzotriazole; [f] PSA = 2-phenylbenzimidazole-5-sulfonate; [g] MXene@LDH:MoO_4^{2-} (1:3); [h] M+G = MoO_4^{2-} + gluconate ($C_{12}H_{22}O_{14}^{2-}$) in (4:1) proportion.

Epoxy coating without filler shows comparable values of modulus of the impedance at the low frequency response of |Z| at 10^{-2}Hz equal to 10^9 Ω.cm^2 (Cao et al., 2022b; Fang et al., 2023) or 4.10^9 Ω.cm^2 (Leal, 2023) to our data |Z| at 10^{-2}Hz = 2.10^9 Ω.cm^2. This makes possible simple comparison at the starting time of the corrosion test and possibly during exposure when the coating thickness as well as the filler loading is also comparable to our data. Also, one should note all the exposure tests reported in table 1 are performed using 3.5 % NaCl solution.

Through the literature, it is remarked that low loading is usually efficient in providing performance in corrosion inhibition and that an increase in filler loading even small has a deleterious effect. For instance as in our case the epoxy coating using Zn_2Al:PSA performs the best using 0.6 wt. % of filler loading while it fails totally at 0.8 wt. %, resulting in a fracture surface due to the filler aggregation (Ding et al., 2023). Such uneven distribution of filler particles leading sometimes to blistering until coating failure is usually observed for slightly higher percentage such as for Mg_2Al:fumarate with 7 wt. % (Zhang et al., 2023) or Ca_2Al:2MBT with 5 wt. % (Tabish et al., 2022). Such drastic effect is also observed in our case at the initial time and even more pronounced after short immersion times (Figure 6). Usually, the percentage of filler loading to obtain the best performance is around 1 to 2 wt. % (Table 1), but some systems require even less but they are using combination of cargos and/or corrosion inhibitors such as Gr@PMIH with 0.5 wt. % (He et al., 2024) or Mg_2Al:MoO_4^{2-} with MXene $Ti_3C_2T_x$ in 0.1 wt. % (Li et al., 2023). In the case of the combination of

compounds, the value of the impedance modulus at lower frequency is highly dependent of the relative ration as found between graphene and polydopamine/$Mg_2Al:MoO_4^{2-}$ (He et al., 2024). Although promising Mg_2Al:BTA, the filler does not improve the inhibition corrosion, incorporated in 1.5 wt. % in epoxy coating, |Z| at 10^{-2}Hz decreases from 10^{11} to 10^9 $\Omega.cm^2$ (Rodriguez et al., 2020). This is interpreted by the presence of defect at the interface filler particles and the epoxy resin leading to the passage of the electrolyte.

Some studies report no EIS data showing Tafel measurement only, as for an epoxy using a combination of 3 wt. % $Zn_2Al:V_{10}O_{28}^{2-}$ functionalized with silane (Aminifazl et al., 2024). Another study reports the use of hybrid sol-gel silane solution with Mmt-Ce and Zn_2Al: DEDTC (Mohammadi et al., 2022) and $Zn_2Al:PO_4^{3-}$@ZIF8 structure was also used a dual-functional carrier (Mohammadkhani et al., 2023).

It is observed that our composite polymer coating with 0.75 wt. % of LDH filler behaves well at the initial time of testing since |Z| at 10^{-2}Hz is one order of magnitude higher than the value obtained using a combination of additives as for Gr@PMIH (He et al., 2024), and LDH:DEDTC with Mmt (Ce) (Mohammadi et al., 2022). When a unique LDH is used, such as for fumarate (Zhang et al., 2023), gallate (Fang et al., 2023), BTA (Rodriguez et al., 2020) or PSA (Ding et al., 2023), our initial |Z| at 10^{-2}Hz data exceeds them by several orders of magnitude from 5 to 1, respectively (Table 2). Indeed |Z| at 10^{-2}Hz obtained here is comparable to the best performing system using 2 wt. % of LDH:NO_2^- in a 120 μm thick-epoxy coating (Xue et al., 2023), while the authors observed a deleterious of $Ca_2Al:MoO_4^{2-}$ with a collapse of the LDH structure in time.

Interestingly a study reports the effect of the cation LDH composition to provide barrier properties (Cao et al., 2022b). As in our case using nitrate form of LDH, the LDH fillers show poor compatibility with the epoxy coating and the reaction of Cl^- ions uptake by the anion-exchange reaction with the interleaved NO_3^- ions is found negligible compared to the barrier effect supplied by the platelets, ranking as follows $Ca_2Al > Zn_2Al > Mg_2Al$ (Table 2). After immersion time up to 21 days, the barrier properties do not change much but only the platelets Ca_2Al do provide an efficient barrier effect when compared to epoxy coating free of filler, Zn_2Al and Mg_2Al show values of |Z| at 10^{-2}Hz lower than EP coating of 10^6 $\Omega.cm^2$ after 21 days (Cao et al., 2022b).

After immersion times into NaCl solution, behaviours differ significantly as |Z| at 10^{-2}Hz or R_{CT} values are found to decrease or to increase.

As in the present case where our composite coating drops from 2.10^{11} to 1.10^{10} Ω.cm^2 after 21 days, the value of |Z| at 10^{-2}Hz for the epoxy coating with LDH:gallate is found to decrease after the same time from 4.10^9 to 1.10^8 Ω.cm^2 (Fang et al., 2023). The decay is even more rapid for MgAl:fumarate where |Z| at 10^{-2}Hz is going down from 10^6 to 2.7 10^5 Ω.cm^2 after 6 days of immersion (Zhang et al., 2023). A decay of about one order of magnitude is usually observed after immersion time as for epoxy using Ca_2Al:2MBT dropping from 5.10^7 to 6.10^6 Ω.cm^2 after 15 days (Tabish et al., 2022) or even two orders of magnitude as for Mg_2Al:BTA after 14 days (Rodriguez et al., 2020) or Zn2Al:PSA from 10^{10} to 10^9 Ω.cm^2 after 21 days (Ding et al., 2023). Some authors use a mixture of carriers such as LHS (Zn based):MoO_4^{2-} and Zn_2Al:$C_{12}H_{22}O_{14}^{2-}$ that efficiently inhibit the progress of corrosion after long-term period as long as 4 months (Leal et al., 2023), however the initial modulus of the impedance is found lower for the composite coating 2.10^8 Ω.cm^2 than for epoxy itself (4.10^9 Ω.cm^2) and this is reverse after 21 days EP and EP composite of 5.10^4 Ω.cm^2 and 2.10^5 Ω.cm^2, respectively. Such long-term properties are explained by the deposition of the corrosion product in the damaged zone, one should note that the inhibitors free of cargo, M+G, behave quite well (Leal et al., 2023). In some cases, |Z| at 10^{-2}Hz is found to increase as for epoxy with Gr@PMIH from 1.6 10^8 to 3.2 10^8 Ω.cm^2 after 21 days, then to decrease after for more prolonged times.

Figure 7 shows the macrographs of the samples after immersion in the neutral chloride solution. Some blisters and/or whitish spots are observed for all samples which could suggest water uptake. For the coating without LDH-EDDS (fig. 7a), there were numerous spots of blisters uniformly distributed all over the entire immersed surface, suggesting some water uptake from the damaged coating. Some reddish-brown spots emphasizing the presence of the corrosion process are also visible. From results and observations presented in figures 6 and 7,

for this coating free of LDH-EDDS, the electrolyte diffuses easily through its thickness without any hindrance causing de-bonding, and consequently early degradation of coating barrier properties (Duval et al., 2002; Le Thu et al., 2006).

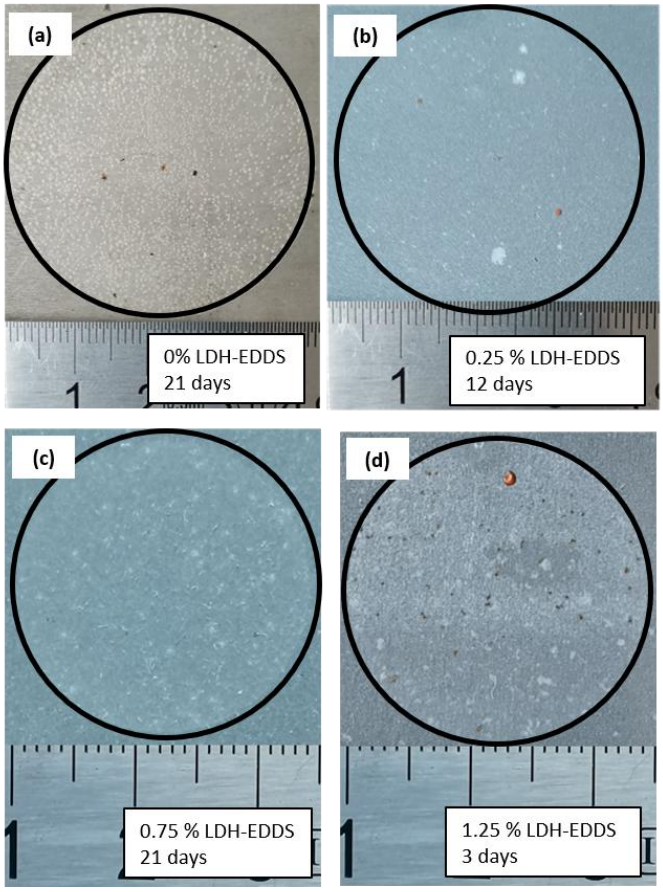

Figure 7: Macrographs of the samples after different immersion times in 0.1M NaCl electrolyte: (a) without LDH, (a) with 0.25 % LDH, (c) 0.75 % LDH and (d) 1.25 % LDH. - containing coating. The black circle marks the surface in contact with the aqueous solution.

When LDH-EDDS is incorporated into the epoxy coating, the surface state is different compared to the coating without LDH-EDDS. Whitish precipitates are observed which could be attributed to the interaction between the electrolyte and the LDH themselves. For 0.25 % LDH-containing coating (Fig. 7b), the whitish spots were less than that of the LDH-free coating, suggesting weaker interactions between epoxy and electrolyte. It is interesting to observe that the whitish spots are distributed randomly compared to the reference. This

suggest that the presence of 0.25 % LDH-EDDS limits the diffusion of electrolyte to some extent and acts locally as inhibitive specie. However, reddish-brown corrosion spots were also observed and attributed to insufficient amount of LDH-EDDS, which could explain the decrease in the impedance modulus after 3 days of immersion (Jagtap et al., 2022). The presence of 0.75% LDH-EDDS gives the highest impedance modulus values after 21 days of immersion, with no colored visible corrosion spots, except some whitish spots (Fig. 7c). This coating demonstrates superior protection in agreement with its impedance modulus which could be attributed to optimum amount of LDH-EDDS (Wang et al., 2019). The surface state of the coated sample containing the highest content of LDH-EDDS is characterized by some black spots of corrosion signatures and a large reddish-brown corrosion product (Fig. 7d). This suggest that 1.25 % LDH-EDDS concentration could cause severe corrosion instead of protection (Jagtap et al., 2022). That could be attributed to LDH-EDDS particles agglomerating together and creating more defects (Cao et al., 2022a). In addition, higher concentration of LDH-EDDS could lead to excessive leaching of EDDS which could cause osmotic pressure and blistering (Wang et al., 2019; Yeganeh et al., 2019). From these results, the best candidate is the coating loaded with 0.75% of LDH-EDDS.

Impedance diagrams obtained for both coated systems immersed in 0.1 M NaCl solution as a function of immersion time are presented in figure 8 in Bode coordinates. The shape of the impedance diagrams at high frequency range indicates a Constant-Phase-Element (CPE) behavior, which is defined by a constant phase angle $\phi < -90°$ (Mahdavian and Attar, 2006). The frequency range attributed to the CPE behavior is smaller for the sample unloaded with LDH (Fig. 8a) compare to the sample containing 0.75% LDH (Fig. 8b). It is interesting to note that the high frequency part of the impedance diagrams remains superimposable with immersion time for both samples. The impedance measurement in low frequency range is not

stationary for the sample containing LDH for immersion time less than 21 days. After this time, the shape of the phase as a function of the frequency is similar to that of the LDH-free sample for shorter immersion times. In parallel, the impedance modulus at low frequency was relatively high for the sample with 0.75% LDH-EDDS (≈ 10^{11}-10^{10} Ω cm²) by comparison with the LDH-free coated plate (≈ 10^{9} Ω cm²), indicating the highest barrier properties for the coating loaded with LDH. The low frequency part of the Bode diagrams is attributed to the carbon steel/electrolyte interface. For epoxy systems, the presence of a Constant-Phase-Element (CPE) is attributed to the presence of pores and/or free volume in the macromolecular network, which lead to hydration of the coating via permeation of the electrolyte through the epoxy matrix.

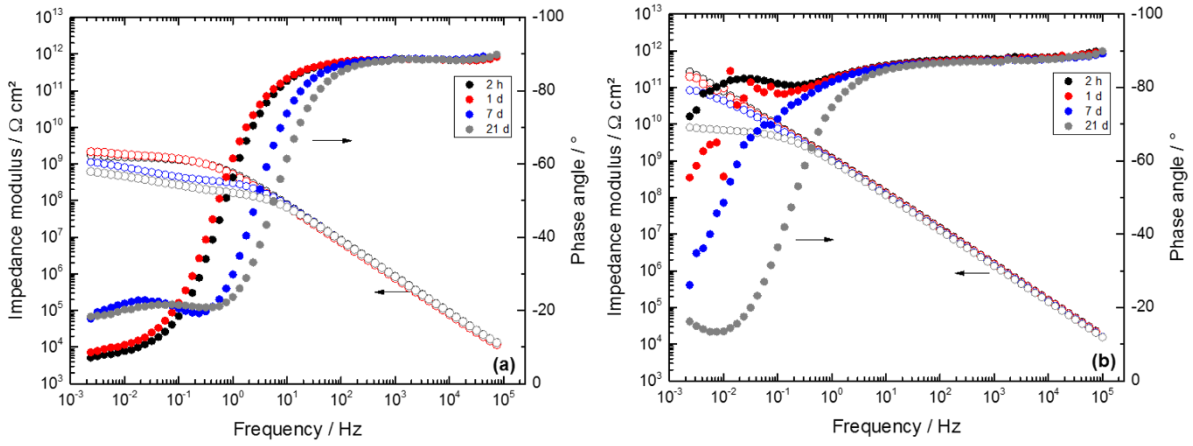

Figure 8: Bode impedance diagrams obtained during time for: (a) the LDH-free and (b) the 0.75%-LDH sample in the 0.1M NaCl solution.

The dielectric properties of epoxy coatings are affected by the hydration of the epoxy matrix during immersion time. Thus, the CPE behavior observed for conventional epoxy coatings has been attributed to a normal distribution of the properties explained by a power law distribution of the resistivity along the coating thickness. The power law model (PLM) proposed by Hirschorn *et al*. (Hirschorn et al., 2010a; Hirschorn et al., 2010b) has been

successfully used for analysis of impedance diagrams for epoxy coatings (Musiani et al., 2014; Nguyen et al., 2015; Nguyen et al., 2016; Amand et al., 2013; Chen t al., 2016). Table 2 summarizes the representative parameters obtained for both coatings using the PLM. The impedance data were fitted from 10^5 Hz to 0.1 Hz. The CPE parameter α was graphically determined from the phase vs frequency representation on the plateau in high frequency range ($\alpha = -\phi / 90°$, (Orazem et al., 2006). The capacitance was graphically determined, and finally the permittivity of the coating was determined using equation 2, with the same procedure as before for the data obtained in dry condition. The resistivity at the interface between the carbon steel and epoxy coatings (ρ_0) was determined by the fitting with Simad software provided by LISE CNRS Paris.

The resistivity at the epoxy coating/electrolyte interface (ρ_δ) was determined using equation 3, where the capacitance is defined as (Hirschorn et al., 2010a):

$$C = gQ(\rho_\delta \varepsilon \varepsilon_0)^{(1-\alpha)} \quad (3)$$

Here,

$$Q = \frac{(\varepsilon \varepsilon_0)^\alpha}{g \delta \rho_\delta^{1-\alpha}} \quad (4)$$

And the function g, depending on α value, allows to adjust the model, is given by:

$$g = 1 + 2.88 \left(\frac{1}{1-\alpha}\right)^{-2.375} \quad (5)$$

α and Q are the CPE parameters, ε is the permittivity of the coating, and ε_0 is the vacuum permittivity. The parameters δ and ω are the coating thickness and the angular frequency, respectively. The swelling by the water uptake is neglected. Thus, the thicknesses δ used to

obtain the resistivity profiles are equal to 80 µm. From resistivities, the frequency domain of application of the model is defined by the characteristic frequencies f_0 and f_δ (Hirshorn et al., 2010a; Hirschorn et al. 2010b):

$$f_0 = \frac{1}{2\pi\rho_0\varepsilon\varepsilon_0} \quad (6)$$

and

$$f_\delta = \frac{1}{2\pi\rho_\delta\varepsilon\varepsilon_0} \quad (7)$$

It appears that the PLM is valid for the domain of frequencies between almost 10^5 Hz and 0.1 Hz. These results clearly indicate that the PLM can be used to analyze the CPE behavior observed for these two coatings. Figure 9 shows the good agreement between the experimental and fitted impedance diagrams.

Table 3: Parameters obtained by graphical method, calculation and by fitting procedure.

Coating	Time	α_c (Hirshorn et al., 2010a)	Q_c /10^{-10} Ω^{-1} cm^{-2} s$^{\alpha}$ (Hirshorn et al., 2010a)	C_∞ /10^{-10} F cm^{-2} from (1)	ε_C from (2)	ρ_δ / 10^5 Ω cm from (4)	α_c by fitting	ρ_δ / 10^5 Ω cm by fitting	ρ_0 / 10^{11} Ω cm by fitting	f_δ / 10^5 Hz from (7)	f_0 /Hz from (6)
0 %	2 h	0.98	2.13	1.61	14.55	6.33	0.98	6.88	1.65	1.8	0.75
	1 d	0.98	2.50	1.81	16.36	0.66	0.98	1.13	1.82	9.7	0.60
	7 d	0.98	2.30	1.77	16.00	1.43	0.98	1.12	0.49	10.0	2.29
	21 d	0.98	2.27	1.61	14.55	2.62	0.98	1.12	0.26	11.0	1.10
0.75 %	2 h	0.98	1.19	9.20	8.31	33.3	0.97	59.2	19.7	0.37	0.11
	1 d	0.98	1.25	9.70	8.77	39.9	0.97	47.6	18.2	0.43	0.11
	7 d	0.98	1.31	1.01	9.13	27.5	0.97	36.4	16.1	0.54	0.38
	21 d	0.98	1.34	1.03	9.31	23.0	0.97	29.9	7.44	0.65	0.26

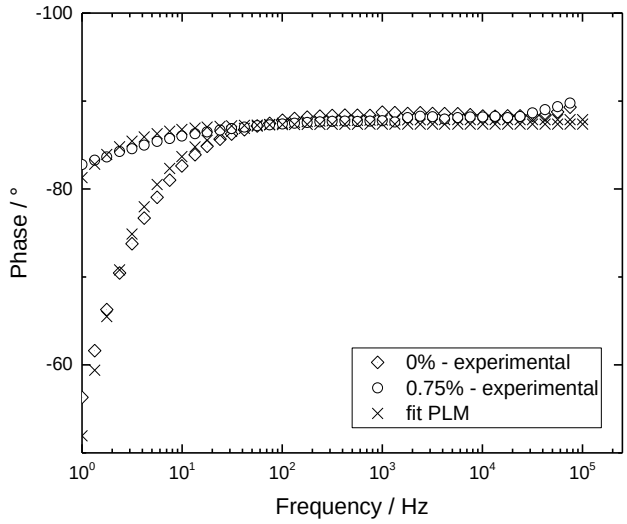

Figure 9: Fit result from power law model for experimental high frequency part of the impedance diagrams obtained after 2 h of immersion for both coatings.

Figure 10 shows the resistivity distribution obtained for both coated samples. The shape of the resistivity profiles similar. The resistivity at coating / electrolyte interface is decreasing with time, but slower for the 0.75% LDH coating. The value of ρ_0 remains higher for the coating loaded with LDH-EDDS (Fig. 10b) by comparison with the reference coating (Fig. 10a). Moreover, the coating thickness characterized by the constant resistivity is higher when the coating contains LDH-EDDS. This behavior can be related to the presence of LDH in the epoxy network, which lead to microstructure variation of the epoxy network (Rodriguez et al. 2020). The permittivity of pure epoxy coatings reaches around 14 immediately after immersion, with only slight variation over time. This means that water penetrates the coating very quickly. In the presence of 0.75% of LDH-EDDS, water uptake is limited from immersion (ε = 8.31) and its kinetics is limited over time; ε reached 9.31 after 21 days of immersion (table 3). It can be related to the presence of LDH which seal the porosities and therefore limits water sorption (Jagtap et al., 2022).

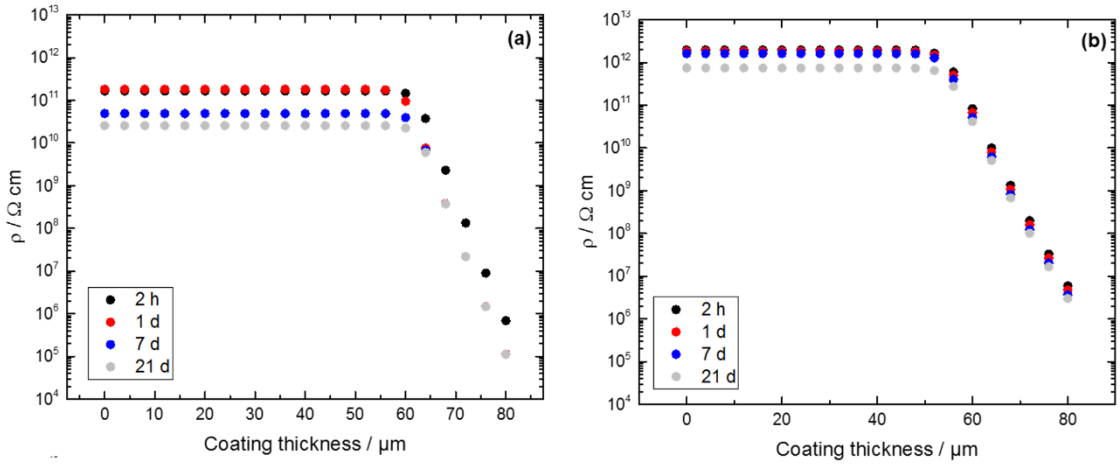

Figure 10: Resistivity distribution in the coatings thicknesses according to a power law: (a) epoxy coating without LDH and (b) with 0.75% of LDH-EDDS.

The experimental approach used is interesting because it allows both the barrier properties of the coating and the reactivity of the coated carbon steel to be considered. However, the electrochemical response is complex to interpret, as the corrosion that develops in steel coated with pure epoxy coating can render the delicate resistivity profile interpretation at the carbon steel/coating interface, characterized by the resistivity ρ_{δ}, which must take into account the local modification of the electrolyte in contact with the carbon steel. However, the values reported in table 3 show that when the epoxy matrix contains 0.75% LDH-EDDS, the barrier properties are improved, mainly by increasing the tortuosity of the polymer network. In addition, once LDH comes into contact with diffusing water, Cl^- ions are captured, slowing down the release of $EDDS^{4-}$ anions, on the one hand, and the subsequent dissolution of $Zn(OH)_2$ hydroxide sheets, on the other hand. These two released species, $EDDS^{4-}$ and Zn^{2+}, under the effect of mass transport, adsorb onto the carbon steel, protecting it from corrosion, as shown in figure 7c after 21 days of immersion in 0.1 M NaCl electrolyte.

The $[Zn_2Al(OH)_6]^+[EDDS]^{4-}_{0.25}$. $2H_2O$ LDH incorporation in epoxy matrix is very interesting by playing a role on three fundamental points in corrosion protection of carbon steel:

- the tortuosity of the polymer network is increasing, delaying the diffusion of water,
- in the chemistry of the electrolyte that diffuses into the polymer network, capturing aggressive ions,
- and as a corrosion inhibitor through its synergistic effect on carbon steel, as shown in previous work (Ayemi et al., 2021).

Figure 11 summarizes the corrosion inhibition mechanism for the sample containing the optimum LDH-EDDS content.

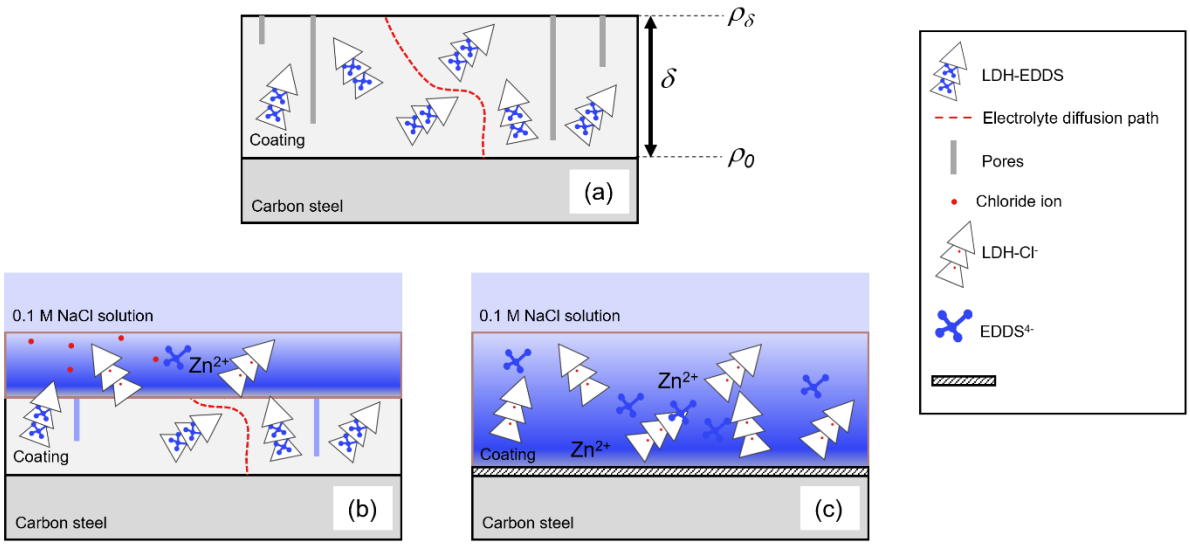

Figure 11: Schematic representation of the corrosion inhibition mechanism offered by LDH-EDDS in epoxy matrix under water-uptake: (a) dry coating, (b) at early stage of immersion and (c) at long immersion time in neutral chloride aqueous solution.

Conclusion

In this work, epoxy systems containing double hydroxide layers $[Zn_2Al(OH)_6]^+[EDDS]^{4-}_{0.25}$. $2H_2O$ were developed as anticorrosive coatings for XC38 carbon steel. The water-barrier properties of these new materials were evaluated using electrochemical impedance measurements performed in a neutral chloride solution. The thicknesses of the coatings were not strictly homogeneous as some defects were visible on the surface of the carbon steel plates. Nevertheless, by selecting the test surface, it was shown that the electrochemical behaviors of the samples were depending on LDH content. The best candidate was the 0.75 % LDH-containing coating, for which the barrier properties were compared to the reference sample (without LDH). The power law model was used and the obtained resistivity profiles showed a higher resistivity at the carbon steel/coating and coating/electrolyte interfaces during time for the LDH-EDDS-loaded coating compared to the one without hybrid filler. The associated value of |Z| at low frequency places Zn_2Al:EDDS as one of the best LDH filler as a protective barrier against the corrosion so far, this without using a combination of compounds and/or sophisticated methods in elaborating its hybrid organic-inorganic framework while keeping a straightforward and sustainable approach. This behavior can be explained by the presence of LDH-EDDS platelets having as an effect to increase the tortuosity of the diffusion paths of water, as well as to capture of Cl^- ions through a combined release of some Zn^{2+} cations and of all the initially interleaved $EDDS^{4-}$ anions, altogether acting in synergy to form an organometallic at the carbon steel surface.

Acknowledgements

The authors acknowledge Petroleum Technology Development Fund (PTDF) Nigeria, for the funding of Gata Joseph Ayemi PhD work.

References

Alibakhshi, E., Ghasemi, E., Mahdavian, M., Ramezanzadeh, B., 2017. A comparative study on corrosion inhibitive effect of nitrate and phosphate intercalated Zn-Al-layered double hydroxides (LDHs) nanocontainers incorporated into a hybrid silane layer and their effect on cathodic delamination of epoxy topcoat. Corros. Sci. 115, 159-174.

Amand, S., Musiani, M., Orazem, M.E., Pébère, N., Tribollet, B., Vivier, V., 2013. Constant-phase-element behavior caused by inhomogeneous water uptake in anti-corrosion coatings. Electrochim. Acta 87, 693-700.

Aminifazl, A., Karunarathne, D.J., Golden, T.D., 2023. Synthesis of Silane Functionalized LDH-Modified Nanopowders to Improve Compatibility and Enhance Corrosion Protection for Epoxy Coatings. Molecules. 29, 819.

Anjum, M.J., Yasin, G., Tabish, M., Malik, M.U. 2020. A Review on Self-Healing Coatings Applied to Mg Alloys and Their Electrochemical Evaluation Techniques. Int. J. Electrochem. Sci. 15, 3040-3053.

Asadi, N., Naderi, R., Mahdavian, M., 2019. Synergistic effect of imidazole dicarboxylic acid and Zn^{2+} simultaneously doped in halloysite nanotubes to improve protection of epoxy ester coating. Prog. Org.Coat.132, 29-40.

Ayemi, G.J., Marcelin, S., Therias, S., Leroux F., Normand, B., 2022. Synergy effect between layer double hydroxide (LDH) and EDDS for corrosion inhibition of carbon steel. Appl. Clay Sci.222, 106497-106507.

Bakhtaoui, N., Benali, O., Mazario, E., Recio, F.J., Herrasti, P., 2021. Layered double hydroxides intercalated with methyl orange as a controlled-release corrosion inhibitor for iron in chloride media. Nano Express, 2, 010017-010028.

Benoit, M., Bataillon, C., Gwinner, B., Miserque, F., Orazem, M.E., Sánchez-Sánchez, C.M., Tribollet, B., Vivier, V., 2016. Comparison of different methods for measuring the passive film thickness on metals. Electrochim. Acta 201, 340-347.

Bouvet, G., Nguyen, D.D., Mallarino, S., Touzain, S., 2014. Amalysis of the non-ideal capacitive behaviour for high impedance organic coatings. Prog. Org. Coat. 77, 2045-2053.

Cao, Y., Zheng, D., Lin, C., 2021. Effect of hysical barrier and anion-exchange process of nitrate-intercalated ZnAl layered double hydroxide films grown on Al n corrosion protection. Surf. Coat. Technol. 421, 127436-.127446

Cao, Y., Zheng, D., Zhang, F., Pan, J., Lin, C., 2022a. Layered double hydroxide (LDH) for multi-functionalized corrosion protection of metals: A review. J. Mater. Sci. Technol. 102, 232-263.

Cao, Y.H., Wang, J.J., Chen, K.F., Zhang, X.Y., Zhang, B., Fang, S., Liang, Y., Huang, C.S., Wang, X.Y., 2022b. A Comparative Study of Chloride Adsorption Ability and Corrosion Protection Effect in Epoxy Coatings of Various Layered Double Hydroxides. Coatings 12, 1631.

Chakri, S., Frateur, I., Orazem, M.E., Sutter, E.M.M., Tran, T.T.M., Tribollet, B., Vivier, V., 2017. Improved EIS analysis of the electrochemical behaviour of carbon steel I alkalne solution. Electrochim. Acta 246, 924-930.

Chen, Y.-M., Nguyen, A.S., Orazem, M.E., Tribollet, B., Pébère, N., Musiani, M., Vivier, V., 2016. Identification of resistivity distributions in dielectric layers by measurement model analysis of impedance spectroscopy. Electrochim. Acta 219, 312-320.

Ding, C.Y., Wu, J.X., Liu, Y., Sheng, X.X., Cheng, X.L., Xiong, X.Y., Zhao, W.L., 2023. A Waterborne Epoxy Composite Coating with Smart Corrosion Resistance Based on 2-Phenylbenzimidazole-5-sulfonic Acid/Layered Double Hydroxide Composite. Molecules. 28, 5199.

Garden, L., Pethrick, R.A., 2017. A dielectric study of water uptake in epoxy resin systems. J. Appl. Polym. Sci.134, 44717.

Duval, S., Keddam, M., Sfaira, M., Srhiri, A., Takenouti, H., 2002. Electrochemical impedance spectroscopy of epoxy-vinyl coating in aqueous medium analyzed by dipolar relaxation of polymer. J. Electrochem. Soc., 149, B520-B529.

Fang, S., Chen, K.F., Yao, H.R., Cao, Y.H., Guo, S.L., Wang, L., Wang, Y.S., Yu, S., Wang, N., 2023. Preparation of Gallic Acid Intercalated Layered Double Hydroxide for Enhanced Corrosion Protection of Epoxy Coatings. Coatings 13, 128.

Hang, T.T.X., Truc, T.A., Olivier, M.-G., Vandermiers, C., Guérit, N., Pébère, N., 2010. Corrosion protection mechanisms of carbon steel by an epoxy resin containing indole-3 butyric acid modified clay. Prog. Org. Coat. 69, 410-418.

Hang, T.T.X., Truc, T.A., Duong, N.T., Pébère, N., Olivier, M.-G., 2012. Layered double hydroxides as containers of inhibitors in organic coatings for corrosion protection of carbon steel. Prog. Org. Coat. 74, 343-348.

He, T., Yuan, Q., Li, H.J., Xie, P., Li, C.H., He, Y., Lin, Y.H., 2024. Waterborne epoxy coating with excellent barrier and self-healing properties for long-term corrosion protection. Inter. J. Electrochem. Sci. 19, 100486.

Hejjaj, C., Ben Razzouq, S., Sahir, Z., Idrissi, A., Bouzakraoui, S., Erramli, H., Fischer, C.B., Alami, J., 2024. Amino acid motif intercalated in an inorganic layered phosphate container for improved steel protection: Experimental and computational evaluation. Colloids Surf. A: Physicochem. Eng. 685, 133266-133277.

Hirschorn, B., Orazem, M.E., Tribollet, B., Vivier, V., Frateur, I., Musiani, M. 2010. Constant-Phase-Element behavior caused by resistivity distributions in films: I. Theory. J. Electrochem. Soc. 157, C452-C457.

Hirschorn, B., Orazem, M.E., Tribollet, B., Vivier, V., Frateur, I., Musiani, M. 2010. Costant-Phase-Element behavior caused by resistivity distributions in films: II. Applications. J. Electrochem. Soc. 157, C458-C463.

Jagtap, A., Wagle, P.G., Jagtiani, E., More, A.P., 2022. Layered double hydroxides (LDHs) for coating applications. JCTR 19, 1-24.

Ju, J.J., Wang, Y., Yu, M.H., Sun, X., Li, W.L., Zhao, Z.B., 2023. Anti-corrosion improvement of epoxy coating by the synergistic effect of barrier shielding and slow-release based on phytic acid intercalated hydrotalcite. J. Appl. Polym. Sci. 140, e54459.

Leal, D.A., Wypych, F., Bruno Marino, C. E., 2020. Zinc-Layered Hydroxide Salt Intercalated with Molybdate Anions as a New Smart Nanocontainer for Active Corrosion Protection of Carbon Steel. ACS Appl. Mater. Interfaces 12, 19823-19833.

Leal, D.A., Sousa, I., Bastos, A.C., Tedim, J., Wypych, F., Marino, C.E.B., 2023. Combination of layered-based materials as an innovative strategy for improving active corrosion protection of carbon steel. Surf. Coat. Techn. 473, 129972.

Le Thu, Q., Takenouti; H., Touzain, S., 2006. EIS characterization of thick flawed organic coatings aged under cathodic protection in seawater. Electrochim. Acta, 51, 2491-2502.

Li, C.H., He, Y., Zhao, Y., Li, Z.J., Sun, D., Li, H.J., Chen, W., Yan, J., Wu, G.Y., Yuan, Xi., 2023. Cataphoretic deposition of an epoxy coating with the incorporation of Ti3C2Tx@Mg-Al layered double hydroxide for long-term active corrosion protection effect. Prog. Org. Coat. 175, 107333.

Mahdavian, M., Attar, M.M., 2006. Another approach in analysis of paint coatings with EIS measurement: Phase angle at high frequencies. Corros. Sci. 48, 4152-4157.

Marcelin; S., Livi, S., Ter-Ovanessian, B., Mary, N. Normand, B., 2024. Potential of epoxy coating containing ionic liquid as anti-corrosion coating: evaluation of barrier properties. Surf. Coat. Technol. 477, 130376-130385.

Mohammadi, I., Shahrabi, T., Mahdavian, M., Izadi, M., 2022. Construction of an epoxy coating with excellent protection performance on the AA 2024-T3 using ion-exchange materials loaded with eco-friendly corrosion inhibitors. Prog. Org. Coat., 166, 106786.

Mohammadkhani, R., Sharifi, K., Fedel, M., Ramezanzadeh, B., 2024. Fabricating epoxy composite coating having self-healing/barrier anti-corrosion functions utilizing ion-exchange/pH-sensitive phosphate-doped ZIF8 MOF decorated Zn-Al-LDH nano-layers. Surf. Coat. Techn. 477, 130284.

Montemor, M.F., 2014. Functional and smart coatings for corrosion protection: A review of recent advances. Surf. Coat. Technol., 258, 17-37.

Musiani, M., Orazem, M.E., Pébère, N., Tribollet, B., Vivier, V., 2014. Determination of resistivity profiles in anti-corrosion coatings from constant-phase element parameters. Prog. Org. Coat. 77, 2076-2083.

Nguyen, A.S., Musiani, M., Orazem, M.E., Pébère, N., Tribollet B., Vivier, V., 2015. Impedance analysis of the distributed resistivity of coatings in dry and wet conditions. Electrochim. Acta 179, 452-459.

Nguyen, A.S., Musiani, M., Orazem, M.E., Pébère, N., Tribollet, B., Vivier, V., 2016. Impedance stufy of the influence of chromates on the properties of waterborne coatings deposited on 2024 aluminium alloy. Corros. Sci. 109, 174-181.

Nguyen, A.S., Causse, N., Musiani, M., Orazem, M.E., Pébère, N., Tribollet, B., Vivier, V., 2017. Determination of water uptake in organi coatings deposited on 2024 aluinium alloy: comparison between impedance measurements and gravimetry. Prog. Orga. Coat. 112, 93-100.

Nguyen, D.T., To, H.T.X., Gervasi, J., Paint, Y., Gonon, M., Olivier, M.-G., 2018. Corrosion inhibition of carbon steel by hydrotalcites modified with different organic carboxylic acids for organic coatings. Prog. Org. Coat. 124, 255-266.

Normand, B., Takenouti, H., Keddam, M., Liao, H., Monteil, G., Coddet, C., 2004. Electrochemical impedance spectroscopy and dielectric properties of polymer: application to PEEK thermally sprayed coating. Electrochim. Acta 49, 2981-2986.

Orazem, M.E., Pébère, N., Tribollet, B., 2006. Enhanced graphical representation of electrochemical impedance data. J. Electrochem. Soc. 153, B129-B136.

Pellanda, A.C., Neto, A.G.C., de Carvalho Jorge, A.R., Berton, M.A.C., Floriano, J.B., Thomas, S., Vijayan, P.P., 2021. Performance evaluation of layered double hydroxides

containing benzotriazole and nitrogen oxides as autonomic protection particules against corrosion. Int. J. Polym. Sci., 2021, 6630194-6630210.

Peng, G., Qiao, Q., Huang, K., Wu, J., Wang, Y., Fu, X., Zhang, Z., Fang, T., Zhang, B., Huang, Y, Li, X., 2020. Ni-Fe-MoO_4^{2-} LDHs/epoxy resin varnish: A composite coating on carbon steel for long-time and active corrosion protection. Prog. Org. Coat. 140, 105514-105524.

Poznyak, S.K., Tedim, J., Rodrigues, L.M., Salak, A.N., Zheludkevich, M.L., Dick, L.F.P., Ferreira, M.G.S., 2009. Novel inorganic host layered double hydroxides intercalated with guest organic inhibitors for anticorrosion applications. ACS Appl. Mater. Interfaces 1, 2353-2362.

Rodriguez, J., Bollen, E., Nguyen, T.D., Portier, A., Paint, Y., Olivier, M.-G., 2020. Incorporation of layered double hydroxides modified with benzotriazole into an epoxy resin for the corrosion protection of Zn-Mg coated steel. Prog.Org. Coat. 149, 105894-105907.

Seniski, A., Monteiro, R.F., Carrera, G.T., d'Orey, M., Bragança, G.P., Portella, 2020. The inhibitory and comparative effects of Zn-Al layered double hydroxide microcontainers intercalated with benzotriazole and nitrite for corrosion protection coatings on AISI 1010 carbon steel. Matéria (Rio de Janeiro) 25.

Su, Y., Qiu, S., Yang, D., Liu, S., Zhao, H., Wang, L., Xue, Q., 2020. Active anti-corrosion of epoxy coating by nitrite ions intercalated MgAl LDH. J. Hazard. Mater. 391, 122215.

Sun, W., Wu, T., Wang, L., Dong, C., Liu, G., 2019. Controlled preparation of MgAl-layered double hydroxide/graphene hybrids and their applications for metal protection. Ind. Eng. Chem. Res. 58, 16516-16525.

Tabish, M., Yasin, G., Anjum, M.J., Malik, M.U., Zhao, J., Yang, Q., Manzoor, S., Murtaza, H., Khan, W.Q., 2021. Reviewing the current status of layered double hydroxide-based smart nanocontainers for corrosion inhibiting applications. J. Mater. Sci. Technol. 10, 390-421.

Tabish, M., Zhao, J., Wang, J.B., Anjum, M.J., Qiang, Y.J., Yang, Q.X., Mushtaq, M.A., Yasin, G., 2022. Improving the corrosion protection ability of epoxy coating using CaAl LDH intercalated with 2-mercaptobenzothiazole as a pigment on steel substrate. Prog. Org. Coat. 165, 106765.

Tedim, J., Kuznetsova, A., Salak, A.N., Montemor, F., Snihirova, D., Pilz, M., Zheludkevich, M.L., Ferreira, M.G.S., 2012. Zn-Al layered double hydroxides as chloride nanotraps in active protective coatings. Corros. Sci. 55, 1-4.

Udoh, I.I., Shi, H., Daniel, E.F., Li, J., Gu, S., Liu, F., Han, E.-H., 2022. Active anticorrosion and self-healing coatings: A review with focus on multi-action smart coating strategies. J. Mater. Sci. Technol. 116, 224-237.

Wang, N., Diao, X., Zhang, J., Kang, K., 2018. Corrosion resistance of waterborne epoxy coatings by incorporation of dopamine treated mesoporous-TiO_2 particles. Coat. 8, 209-223.

Wang, N., Gao, H., Zhang, J., Li, L., Fan, X., Diao, X., 2019. Anticorrosive waterborne epoxy (EP) coatings based on sodium tripolysphosphate-pillared layered double hydroxides (STPP-LDHs). Prog. Org. Coat. 135, 74-81.

Wei, J., Xu, J., Mei, Y.,Tan, Q., 2020. Chloride adsorption on aminobenzoate intercalated layered double hydroxides: Kinetic, thermodynamic and equilibrium studies. Appl. Clay Sci. 187, 105495-105503.

Xie, P., He, Y., Zhong, F., Zhang, C., C.L., Li, H.J., Liu, Y., Bai, Y., Chen, J.Y., 2021. Cu-BTA complexes coated layered double hydroxide for controlled release of corrosion inhibitors in dual self-healing waterborne epoxy coatings. Prog. Org. Coat. 153, 106164.

Xing, X.T., Sui, Y.T., Li, Q.S., Yuan, M., Zhao, H.T., Zhou, D., Chu, X.M., Liu, S.J., Tang, E.J., 2024. Multifunctional ZnAl-MoO4 LDH assembled Ti3C2Tx MXene composite for active/passive corrosion protection behavior of epoxy coatings. Appl. Surf. Sci. 623, 157092.

Xue, J., Cao, Y., Zhang, X., Zhang, L., Chen, K., Huang, C., 2023. Corrosion Protection Mechanism Study of Nitrite-Modified CaAl-LDH in Epoxy Coatings. Coatings. 7, 1166.

Yeganeh, M., Asadi, N., Omidi, M., Mahdavian, M, 2019. An investigation on the corrosion behavior of the epoxy coating embedded with mesoporous silica nanocontainer loaded by sulfamethazine inhibitor. Prog. Org. Coat. 128, 75-81.

Zhang, D., Zhang, H., Zhao, S., Li, Z., Hou, S., 2019. Electrochemical impedance spectroscopy evaluation of corrosion protection of XC35 carbon steel by hyallosite nanotube-filled epoxy composite coatings in 3.5% NaCl solution. Int. J. Electrochem. Sci. 14, 4659-4667.

Zhang, J., Zhao, J.M., Wang, J.B., Tabish, M., Zhang, J.F., 2023. Enhancing the corrosion resistance of waterborne epoxy coating by fumarate intercalated LDHs prepared by high gravity technology. Prog. Org. Coat. 174, 107271.

Zheludkevich, M.L., Poznyak, S.K. Rodrigues, L.M., Raps, D., Hack, T., Dick, L.F., Nunes, T., Ferreira, M.G.S., 2010. Active protection coatings with layered double hydroxides nanocontainers of corrosion inhibitor. Corros. Sci. 52, 602-611.